*Original*

Yang, J.; Khan, M.; Zhang, L.; Ren, X.; Guo, J.; Feng, Y.; Wei, S.; Zhang, W.:
**Antimicrobial surfaces grafted random copolymers with REDV peptide beneficial for endothelialization**
In: Journal of Materials Chemistry B (2015) Royal Society of Chemistry

DOI: 10.1039/c5tb01155h

Journal of
Materials Chemistry B

PAPER

View Article Online
View Journal



Cite this: DOI: 10.1039/c5tb01155h

# Antimicrobial surfaces grafted random copolymers with REDV peptide beneficial for endothelialization†

Jing Yang,‡[a] Musammir Khan,‡[a] Li Zhang,[b] Xiangkui Ren,[ab] Jintang Guo,[ab] Yakai Feng,*[abcd] Shuping Wei[e] and Wencheng Zhang*[e]

Received 15th June 2015,
Accepted 18th August 2015

DOI: 10.1039/c5tb01155h

www.rsc.org/MaterialsB

Polycarbonate urethane (PCU) elastomeric materials have been developed for vascular prosthesis applications, because of their excellent mechanical and physical properties. However, thrombosis and inflammation often limit their usage as small-diameter vascular grafts. Herein, we focused on the design and functionalization of a PCU elastomer with enhanced hemocompatibility, rapid endothelialization and antimicrobial properties. An atom transfer radical polymerization (ATRP) technique was utilized to graft random copolymers of *N*-(2-hydroxypropyl)methacrylamide (HPMA) and eugenyl methacrylate (EgMA) onto a PCU surface, and subsequently the cysteine-terminated CREDV peptide sequence was directly linked onto the surface by a thiol–ene click reaction to prepare a series of REDV peptide functionalized surfaces. The chemical compositions of the modified surfaces were quantified by X-ray photoelectron spectroscopy (XPS), and the hydrophilicity was evaluated by water contact analysis and water uptake. The surface hemocompatibility was verified by platelet adhesion assays, and the results demonstrated that platelet adhesion was significantly reduced on the modified surface. More importantly, the functionalized surfaces with high hydrophilicity and cell specific adhesive REDV peptide could selectively enhance the adhesion and proliferation of human umbilical vein endothelial cells (HUVECs) but they suppressed these behaviors in human arterial smooth muscle cells (HASMCs). Moreover, these surfaces showed excellent antibacterial properties, which originate from the EgMA moieties of the copolymers. The successful fabrication of multifunctional surfaces with excellent hemocompatibility, rapid endothelialization, and good antimicrobial activity through a feasible route could be an attractive platform for tissue engineering applications.

## 1. Introduction

Cardiovascular diseases have become one of the leading causes of death in the world, and the design and application of cardiovascular implants such as stents and vascular grafts have attracted considerable attention with respect to the treatment of these diseases.[1–3] Polyurethane elastomers have been widely applied in cardiovascular implants, such as cardiac pacemakers, left ventricular assist devices, total artificial hearts, and small caliber vascular grafts, due to their good biocompatibility and satisfactory mechanical and physical properties.[4,5] However, the risks of inadequate hemocompatibility, restenosis, thrombosis and infections limit their ultimate success in clinical long-term implantations.[6–8] When the artificial cardiovascular grafts are implanted, their surfaces are in direct contact with blood and they are often recognized as foreign substances by the immune system; this is likely to activate the blood coagulation system and cause inflammatory reactions.[9] The triggered coagulation cascades (namely protein conformation transformation, platelet adhesion and activation, clot formation and dysfunction of fibrinogen) disturb endothelialization and finally lead to restenosis and thrombosis.[10]

It has been postulated that surface wettability and an overall neutral charge are essential properties for efficient resistance to protein adsorption.[11,12] To reduce the interactions of blood components, especially the plasma proteins and platelets,

[a] School of Chemical Engineering and Technology, Tianjin University, Tianjin 300072, China. E-mail: yakaifeng@tju.edu.cn
[b] Tianjin University Helmholtz-Zentrum Geesthacht, Joint Laboratory for Biomaterials and Regenerative Medicine, Weijin Road 92, 300072 Tianjin, China
[c] Key Laboratory of Systems Bioengineering, Ministry of Education, Tianjin University, Tianjin 300072, China
[d] Collaborative Innovation Center of Chemical Science and Chemical Engineering (Tianjin), Weijin Road 92, Tianjin 300072, China
[e] Department of Physiology and Pathophysiology, Logistics University of Chinese People's Armed Police Force, Tianjin 300162, China

† Electronic supplementary information (ESI) available. See DOI: 10.1039/c5tb01155h

‡ These authors have contributed equally to this work.

with the exposed material surface and to improve the hemocompatibility of the polycarbonate urethane (PCU), we had modified PCU with poly(ethylene glycol), zwitterionic polymers, silk-fibroin, heparin, and gelatin by blend electrospinning or surface grafting techniques.[13–29]

Poly[*N*-(2-hydroxypropyl) methacrylamide] (PHPMA) and its copolymers have been widely applied for the delivery of drugs, genes and adenoviruses because of their good water-solubility, stability in aqueous media, biocompatibility, nontoxicity and nonimmunogenicity.[30–32] Furthermore, PHPMA can effectively resist protein adhesion in single plasma proteins; moreover, it shows unprecedentedly low fouling in undiluted blood plasma. Importantly, PHPMA is comparable or even better than the commonly considered ultra-low fouling polymers.[33,34]

Besides hemocompatibility problems, restenosis and thrombosis could also occur on artificial vascular grafts when smooth muscle cells (SMCs) undergo rapid and unregulated adhesion and proliferation over endothelial cells (ECs) and when re-endothelialization is delayed.[35] Because ECs form the innermost layer of the entire vascular system *in vivo*, they play a key role in forming a nonthrombogenic surface.[6] Rapid endothelialization is beneficial for the formation of a confluent, robust layer of functional ECs, and it provides a potential strategy for success in the long-term treatment of cardiovascular diseases.[36] Based on this understanding, many methods have been developed to promote the endothelialization of biomaterial surfaces.[37,38] The extracellular matrix (ECM) proteins, collagen, fibronectin and tropoelastin, have been used to enhance the adhesion and migration of ECs.[6,39,40] Furthermore, many researchers have investigated various peptide sequences derived from ECM such as RGD, REDV, YIGSR, and CAG. These peptide sequences have been used to modify cardiovascular implant surfaces to allow them to directly interact with cell receptors and promote the adhesion, migration and proliferation of ECs.[7,41–46] Among these, RGD is to date the most widely employed peptide sequence for modifying artificial vascular scaffolds. Numerous studies have demonstrated that RGD peptide can enhance the adhesion, spreading and proliferation of ECs on the functionalized surfaces. However, the RGD modified surfaces often show increased platelet adhesion, and the adhered platelets have spread morphology.[47,48] On the other hand, REDV peptide is a well-known EC-selective adhesive peptide, which can specifically bind to the abundant receptors on ECs. However, SMCs rarely have the specific receptors for REDV adhesion.[49] The selective adhesion of ECs over SMCs is attracting increasing attention for the use of REDV peptide in the surface modification of artificial vascular grafts and gene carriers.[50–53] In addition, other investigators have immobilized antibodies, growth factors, proteins and genes to improve the interaction of implants with ECs to accelerate endothelialization.[38,51,54–59]

Infections have become one of the main causes of patient morbidity and mortality.[60,61] In particular, infections caused by surface-bound bacterial cells are a major problem in clinical surgeries and implantation operations.[8] Moreover, infections can also trigger inflammatory reactions and coagulation cascades, narrowing the luminal volume and resulting in restenosis and thrombosis.[62] Thus, antimicrobial and anti-inflammatory properties should be taken into consideration in designing and preparing artificial vascular implants. The commonly utilized antimicrobial agents include quaternary ammonium compounds, small molecular weight antibiotics, and plant-derived antimicrobial agents.[8,63–65] One example is eugenol, which has been popular for its analgesic and anti-inflammatory properties, antimicrobial activity, antipyretic activity and antianaphylactic properties.[66,67] The acrylate derivative of eugenyl methacrylate (EgMA) can covalently link eugenol to macromolecular chains without decreasing its natural properties.[68,69] EgMA-based copolymers have been demonstrated to have high inhibitory effect on bacterial growth.[68]

An ideal cardiovascular implant should possess excellent hemocompatibility, directing the fate of vascular cells, as well as anti-infective and anti-inflammatory properties.[54] Herein, we developed a biomimetic multifunctional surface by grafting hydrophilic HPMA, antimicrobial EgMA, and EC adhesive peptide REDV. First, we used activators that were regenerated by electron transfer atom transfer radical polymerization (ARGET ATRP) technique to graft random copolymers of HPMA and EgMA in different molar ratios onto a PCU surface. Then, the cysteine-terminated peptide CREDV was immobilized on the terminated allyl group of EgMA *via* a thiol–ene click reaction. By varying the molar ratios of hydrophilic HPMA and EC-selective REDV peptide, an optimized biomimetic multifunctional surface was obtained with excellent hemocompatibility and antimicrobial properties, which is beneficial with respect to selective endothelialization on the PCU surface. This modification process is relatively convenient and effective and can be used to create a multifunctional surface for other biomaterials.

## 2. Materials and methods

### 2.1. Materials

Eugenol (99%), methacryloyl chloride (98%), 1-aminopropan-2-ol (92%), α,α-dimethoxy-α-phenylacetophenone (DMPA, 99%), 5,5′-dithio-bis(2-nitrobenzoic acid) (DTNB, 98%) and ascorbic acid (99%) were obtained from Tianjin Heowns Biochemical Technology Co., Ltd. Cysteine-terminated peptide CREDV was purchased from GL Biochem. (Shanghai) Ltd. PCU (Chronoflex C, $M_n$ = 110 kDa) was purchased from Cardio International Inc., USA. 2,2′-Bipyridine (bpy, 99%), Cu(II)$Br_2$ (99.999%), 2-bromoisobutyryl bromide (BIBB, 98%) and ethyl-2-bromoisobutyrate (EBIB, 98%) were purchased from Sigma-Aldrich and used as received. Fluorescein diacetate (FDA) was obtained from Sigma-Aldrich. The orange cell-tracker dye 5-(and 6)-(((4-chloromethyl)-benzoyl)-amino)-tetramethyl-rhodamine (CMTMR) was purchased from Molecular Probes. All other chemicals and solvents were of analytical grade. The solvents were dried and purified by conventional procedures and distilled before use.

### 2.2. Modification and functionalization of PCU-film

**2.2.1. Preparation of PCU-*g*-poly(HPMA-*co*-EgMA) surfaces by ARGET ATRP.** HPMA and EgMA monomers were synthesized and purified using previously reported methods.[32,66] The PCU-film

 

(3 cm × 3 cm) was prepared by solution casting and immobilized BIBB initiator according to our previous method.[63,70] First, PCU-films were treated with hexamethylene diisocyanate with DBTDL as the catalyst at 50 °C for 90 min. After immersing in water for 12 h, the amino group terminated PCU-films were prepared. Subsequently, 5 pieces of the amino group terminated PCU-films were placed in 50 mL dry *n*-hexane with pyridine (1 mL) as the catalyst and the mixture was cooled to −5 °C. Under a nitrogen atmosphere, 1.5 mL BIBB initiator (in 10 mL *n*-hexane) was added dropwise with constant stirring for 1 h. The reaction was further stirred at 25 °C for 6 h. The obtained films were cleaned subsequently with *n*-hexane, ethanol and pure water for 12 h. Then, the films were dried in vacuum at 50 °C for 24 h.

The preparation of PCU-*g*-poly(HPMA-*co*-EgMA) surface was carried out by an ARGET ATRP procedure: a total 10 mmol of HPMA and EgMA mixtures with different molar ratios (4/0, 3/1, 2/2, 1/3, and 0/4) were dissolved in 15 mL mixed solvent (DMSO : $H_2O$, v/v = 1/3) containing $CuBr_2$ (6.7 mg, 0.03 mmol), bpy (31.2 mg, 0.2 mmol) and EBIB (14.7 μL, 0.1 mmol). The mixture was purged with nitrogen for 1 h with continuous stirring. Then, a piece of the initiator-immobilized PCU-film was dropped into the reaction tube at 30 °C. Subsequently, ascorbic acid (44 mg, 0.25 mM in 1 mL $H_2O$), purged with nitrogen for 10 min, was added dropwise using a degassed syringe at 20–30 min intervals for 4 h. The samples were rinsed and incubated in $H_2O$ for 10 h to remove the unconnected reagents. After drying in a vacuum oven overnight, a series of surface modified PCU-films were obtained, namely, PCU-*g*-poly(HPMA4-*co*-EgMA0), PCU-*g*-poly(HPMA3-*co*-EgMA1), PCU-*g*-poly(HPMA2-*co*-EgMA2), PCU-*g*-poly(HPMA1-*co*-EgMA3) and PCU-*g*-poly(HPMA0-*co*-EgMA4), where the numbers indicate the HPMA and EgMA molar ratios in the feed. These were abbreviated as H, H3E1, H2E2, H1E3 and E surfaces, respectively. Moreover, a PCU blank was also used as a control group in the following studies.

**2.2.2. Immobilization of REDV peptide by click reaction.** Cysteine-terminated peptide CREDV (57 mg, 0.080 mmol), DMPA (2.1 mg, 0.0082 mmol) and a piece of allyl group terminated PCU film were added in 10 mL DMF on a transparent glass plate. A click reaction was carried out at 30 °C in a nitrogen atmosphere for 30 min under the exposure of a 365 nm UV lamp (300 W) from a distance of 30 cm. After 15 min, the light source was turned off and the film was turned over. The light was then turned on for another 15 min to treat the other side of the film. After completion of the reaction, the film was cleaned ultrasonically with phosphate buffered saline (PBS, pH = 7.4) to remove the physisorbed peptide, dried under vacuum at 30 °C overnight and stored at −20 °C. REDV peptide functionalized surfaces, denoted as H3E1-REDV, H2E2-REDV, H1E3-REDV and E-REDV, were obtained from H3E1, H2E2, H1E3 and E surfaces, respectively.

### 2.3. Characterization

**2.3.1. Surface chemical composition.** The surface chemical compositions of the PCU-*g*-poly(HPMA-*co*-EgMA) surfaces (H, H3E1, H2E2, H1E3 and E surfaces) and the PCU blank were studied by X-ray photoelectron spectroscopy (XPS) on a PHI-1600 instrument with a Mg Kα X-ray source at $2 \times 10^{-8}$ Torr. Low-resolution survey scans were performed at 187.85 eV in steps of 0.8 eV, and high-resolution survey scans were performed at a pass energy of 29.35 eV in steps of 0.25 eV. Core-level signals were obtained at a photoelectron take-off angle of 45°, and C 1s spectrum bands were deconvoluted into sub-peaks using the XPS PEAK41 software. The experiment was conducted in triplicate.

**2.3.2 Quantification of immobilized REDV peptide.** The concentrations of immobilized CREDV peptide on the modified PCU-films were determined by Ellman's method.[70–73] Briefly, the CREDV stock solution (100 μL, 0.08 mmol) was diluted in 2.5 mL of 0.5 M PBS (pH = 8.0) and reacted with 2.5 mL of Ellman's reagent (DTNB, 0.02 mmol in pH = 8.0 PBS). The absorbance of the reaction mixture at 412 nm ($A_{412s}$) was continuously determined until it reached a constant value, with PBS as a control. In parallel, the CREDV stock solution (100 μL, 0.08 mmol) was diluted in 5 mL of 0.5 M PBS (pH = 8.0) but without DTNB and the absorbance was measured to obtain $A_{412r}$ as the reagent blank. In another control, 0.02 mmol DTNB was diluted in 5 mL 0.5 M PBS (pH = 8.0) and its absorbance was determined as $A_{412c}$. The sulfhydryl group concentration in the CREDV solution was calculated according to the following formula with the standard value $\varepsilon_{412}$ = 14 150 $M^{-1}$ $cm^{-1}$:[73]

$$[SH] = (A_{412s} - A_{412r} - A_{412c})/(\varepsilon_{412} \times 1\ cm)$$

where $A_{412s}$ is the absorbance of CREDV solution in the presence of DTNB, $A_{412r}$ is the absorbance of CREDV solution without DTNB, and $A_{412c}$ is the absorbance of DTNB solution. The results were obtained from three parallel experiments. The immobilized CREDV peptide on the surfaces was calculated from the sulfhydryl group concentrations of the solutions before and after surface modification and the physically adsorbed peptide was collected after washing with PBS.

**2.3.3 Water contact angle (WCA) measurement.** Wettability changes of the modified PCU-films, namely, the PCU-*g*-poly(HPMA-*co*-EgMA) surfaces (H, H3E1, H2E2, H1E3, and E surfaces), the REDV peptide functionalized surfaces (H3E1-REDV, H2E2-REDV, H1E3-REDV and E-REDV surfaces), and the PCU blank were characterized by static WCA measurement using the sessile drop technique with 3 μL distilled water at room temperature on a Kruss Easy Drop goniometer (Kruss, Hamburg, Germany) equipped with a digital photoanalyzer. Contact angles were obtained as an average from six measurements. Three specimens of each film were tested at two different locations and then the average contact angle was calculated from them.

**2.3.4. Water uptake test.** Water uptake (WU) of the PCU-*g*-poly(HPMA-*co*-EgMA) surfaces (H, H3E1, H2E2, H1E3 and E surfaces), the REDV peptide functionalized surfaces (H3E1-REDV, H2E2-REDV, H1E3-REDV, and E-REDV), and the PCU blank control was tested. The pre-weighed samples ($w_0$) were incubated in PBS (pH 7.4) at 37 °C for 24 h. Then, after collecting and drying with a filter paper, they were re-weighed as $w_1$.

The percentage of WU was calculated according to the following formula:

$$WU = (w_1 - w_0)/w_0 \times 100\%$$

WU values were calculated from three parallel experiments.

### 2.4. Platelet adhesion test

The hemocompatibility of the modified PCU-films, namely, H, E, H3E1-REDV, H2E2-REDV, H1E3-REDV, and E-REDV, as well as the PCU blank was detected using a platelet adhesion experiment. For this study, fresh blood was collected from a healthy human volunteer (Tianjin Hospital of Armed Police Forces, Tianjin, China) and stored in a disposable vacuum blood collection tube (EDTA-2K, Guangzhou Improve Medical Technology Co., Ltd). The blood was centrifuged at 1500 rpm at 37 °C for 15 min to prepare platelet-rich plasma (PRP). The PCU-films were placed in 24-well tissue culture plates and immersed in PBS (pH 7.4) for 12 h, and then incubated in PRP at 37 °C for 2 h. After rinsing with PBS three times to remove any non-adhered platelets, the films were placed in 2.5 wt% glutaraldehyde in PBS to fix the adhered platelets for 30 min. Then, the samples were dehydrated with a series of graded alcohol–water solutions (50%, 70%, 80%, 90% and 100%) for 30 min per step and dried under vacuum at 25 °C. All the films were coated with gold for scanning electron microscopy (SEM) examination (S-4800, HI-9053-0003). Platelet attachment was quantified by acquiring 6 random images from three parallel experiments and evaluated by ImageJ software.

### 2.5. Cell culture

Human umbilical vein endothelial cells (HUVECs) were purchased from Allcells Biomart (Shanghai) and cultured in high glucose DMEM supplemented with 10% FBS in an incubator (37 °C, 5% $CO_2$). The cell culture medium for human arterial smooth muscle cells (HASMCs) was RPIM 1640 (Gibco, USA) supplemented with 10% FBS, 100 U $mL^{-1}$ penicillin and 100 μg $mL^{-1}$ streptomycin. Fresh culture medium was changed every other day until the cells reached 90% confluence. Then, the cells were trypsinized to subculture according to the standard techniques. The cell densities for all the experiments were precisely calculated by a hematocytometer and all the samples were sterilized with UV radiation for 30 min before the cell studies.

The adhesion, spread and proliferation of HUVECs and HASMCs on different PCU-films, namely, the PCU blank, H, E, H3E1-REDV, H2E2-REDV, H1E3-REDV, and E-REDV surfaces, were investigated by the FDA assay. Briefly, cells were seeded at a density of $1 \times 10^4$ cells per well in 200 μL complete medium on different PCU-films in 96-well tissue culture plates and the medium was replaced every other day. At pre-determined time points (1, 3 and 7 day), the samples in the tissue culture plates were analyzed by the FDA assay method. Briefly, FDA solution (5 mg $mL^{-1}$ in acetone) was added to the medium, and the cells were further cultured for 15 min. Then, they were washed with D-Hanks solution three times. The adhered cells were stained with FDA and images were obtained by fluorescence microscopy (Fluorescence Olympus U-RFLT50 and Olympus DP72 microscopes). Six random images were selected from three parallel experiments at 20× magnification. The cell density and surface coverage on different surfaces were calculated by the Image-Pro Plus software.

An MTT assay was used to investigate the cell metabolic activity (viability) of HUVECs and HASMCs on the modified PCU-films. 20 μL MTT (5 mg $mL^{-1}$ in 0.01 M, pH 7.4 PBS) solution was added into each well at the pre-determined time point (3 day). After 4 h of incubation at 37 °C, the medium was removed and 150 μL DMSO was added to dissolve the insoluble formazan crystals with shaking for 10 min. The absorbance at 490 nm was determined using a microplate reader (Bio-Rad, IMARK™), and the cell viability as a percentage relative to the untreated control cells was calculated from OD490. All the results were obtained from four parallel measurements.

### 2.6. Co-culture of HUVECs and HASMCs

The competitive adhesion of HUVECs and HASMCs was performed according to a previously reported protocol.[74] Briefly, after the cells were completely detached from the cell-culture flasks, the cell suspensions were centrifuged at 1000 rpm for 10 min and washed twice with D-Hanks solution. The cells were re-suspended in fresh media with the addition of cell-tracker dyes (FDA and CMTMR) for 30 min; then, HUVECs and HASMCs were stained green and red, respectively. The stained cells were centrifuged, resuspended and adjusted to a concentration of $2 \times 10^5$ cells per mL. The two types of cells with the same volume of cell suspensions were mixed together, forming a final concentration of $1 \times 10^5$ cells per mL for each cell, and seeded onto the modified PCU-films in 24-well tissue culture plates at a density of $1 \times 10^5$ cells per well. The competitive adhesion of the two types of cells was observed by a fluorescent microscope after 2 h of incubation (Fluorescence Olympus U-RFLT50 and Olympus DP72 microscopes). All the experiments were performed at least twice and 6 images were obtained for each sample at each channel. The Image-Pro Plus software was used to determine the number of cells.

### 2.7. Surface antibacterial assay

The antibacterial activity of the modified PCU-films, namely, H, E, H3E1-REDV, H2E2-REDV, H1E3-REDV, and E-REDV, as well as the PCU blank was qualitatively and quantitatively evaluated *in vitro* against bacterial inocula (*E. coli*).[63,75,76] *E. coli* were precultured overnight in a Luria-Bertani (LB) liquid medium and subcultured in a fresh medium until the mid-log phase (OD600 = 0.5, where OD600 is the optical density of a sample measured at a wavelength of 600 nm). The nutrient agar was prepared from the LB liquid medium containing 1.5% agar. After autoclaving for 30 min, the agar solution was poured into 100-mm diameter Petri dishes for the subsequent tests.

In the qualitative method, LB-agar plates were prepared and allowed to dry. Then, 1 μL of the diluted strain suspension ($1 \times 10^8$ CFU $mL^{-1}$) was dropped at eight different places on the surface of each agar plate and allowed to absorb. Subsequently, disc samples (6.0 mm diameter), which were first sterilized with

 

UV radiation for 30 min, were placed on top of the bacterial spots. The bacterial spot without films was used as a blank control. The plates were incubated at 37 °C for 24 h. Each polymer disk was visually inspected for colony formation. Three replicates were tested for each sample.

In the quantitative method, the sub-cultured inoculum (*E. coli*) was diluted to a final concentration of $1 \times 10^6$ CFU $mL^{-1}$. 30.0 μL of the bacterial suspension was dropped on the surface of each film and incubated at 25 °C for 3 h. After incubation, 10.0 μL of the inoculum was withdrawn and spread on agar plates; the colonies formed were imaged and counted by the Image-Pro Plus software. The remaining bacterial suspension and samples were immersed in 2.0 mL fresh LB medium and further incubated overnight for optical density measurement by OD600 using a Cary Eclipse fluorescence spectrometer.[61,64] Three parallel measurements were carried out for each sample.

### 2.8. Statistical analysis

Data are represented as mean ± SD (standard deviation of the mean value) unless indicated otherwise and compared by one-way ANOVA tests *via* the Origin 8.0 software (MicroCal, USA). A *P*-value less than 0.05 was considered statistically significant.

## 3. Results

To specifically enhance endothelialization on biomaterial surfaces, we prepared surface modified PCU-films with multiple functions including resistance against non-specific adsorption of proteins and specific recognition of ECs as well as antibacterial properties. The PCU-films were first grafted with random copolymers of HPMA and EgMA with different monomer ratios *via* a very versatile method of living polymerization, ARGET ATRP (Scheme 1). The hydrophilic monomer HPMA was applied herein to improve the hemocompatibility and resistance against non-specific adhesion of proteins, platelets and blood cells. Moreover, EgMA monomer acted mainly as the antimicrobial moiety and its polymers provided many pendant double bonds for covalently linking cysteine-terminated CREDV peptide by photo-initiated thiol–ene click chemistry. By adjusting the ratios of HPMA and EgMA in the feed, we prepared a series of poly(HPMA-*co*-EgMA) and poly(HPMA-*co*-EgMA)-REDV modified PCU surfaces with selective adhesion for ECs and antimicrobial activity.

### 3.1. Surface modification of PCU-films

HPMA and EgMA were grafted onto PCU-films with monomer ratios of 4 : 0, 3 : 1, 2 : 2, 1 : 3 and 0 : 4 by ARGET ATRP. Ascorbic acid was used as a strong reducing agent in the reaction with the aim of quickly converting Cu(II) to Cu(I). Thus, a low concentration of Cu species was needed.[77]

Surface chemical compositions of different PCU-films were analyzed by XPS and the results are summarized in Table 1. The basic peaks of C 1s, O 1s and N 1s indicated C, O and N as the major elements. In the C 1s narrow spectrum of the PCU blank (Fig. 1), C–H, C–N and O=C–O peaks were found at 284.7 eV, 286.4 eV and 289.7 eV, respectively. After grafting of PHPMA (H), the C 1s narrow scan of the H surface showed C–H, C–O and C–N peaks at 284.1 eV, 285.2 eV and 286.4 eV, respectively. The high intensity of the C–O peak confirmed the successful grafting of PHPMA onto the PCU surface. C–H, C–O, C–N and O=C–O peaks of the H2E2 surface were found at 284.7 eV, 285.5 eV, 286.3 eV and 289.4 eV, respectively.

Considering REDV peptide as an EC adhesive peptide, we conjugated the cysteine-terminated CREDV peptide with the pendant double bonds on the modified PCU-films by photo-initiated thiol–ene click chemistry. The amount of immobilized REDV peptide on the modified surfaces was determined by Ellman's method:[73] the total sulfhydryl group (–SH) concentration of the stock peptide solution was first determined. Then, after click reaction with different PCU surfaces, the remaining –SH

Table 1 XPS chemical compositions of different PCU surfaces

| Sample ID | Chemical structure | C 1s (%) | O 1s (%) | N 1s (%) | C/N |
|---|---|---|---|---|---|
| PCU blank | PCU | 69.4 | 28.5 | 2.1 | 33.0 |
| H | PCU-*g*-PHPMA (4 : 0) | 68.5 | 16.4 | 15.1 | 4.5 |
| H3E1 | PCU-*g*-poly(HPMA3-*co*-EgMA1) (3 : 1) | 69.0 | 17.9 | 12.8 | 5.4 |
| H2E2 | PCU-*g*-poly(HPMA2-*co*-EgMA2) (2 : 2) | 69.3 | 19.0 | 11.2 | 6.2 |
| H1E3 | PCU-*g*-poly(HPMA1-*co*-EgMA3) (1 : 3) | 69.7 | 19.5 | 10.7 | 6.5 |
| E | PCU-*g*-PEgMA (0 : 4) | 71.2 | 18.4 | 9.5 | 7.4 |

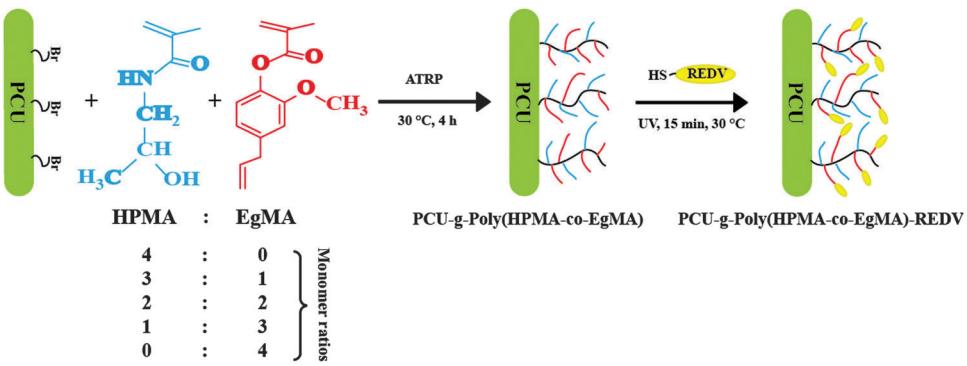


Scheme 1 Surface grafting of HPMA and EgMA copolymers by ATRP at different monomer ratios; the terminated allyl groups were functionalized with cysteine-terminated CREDV peptide by photo-initiated thiol–ene click chemistry.

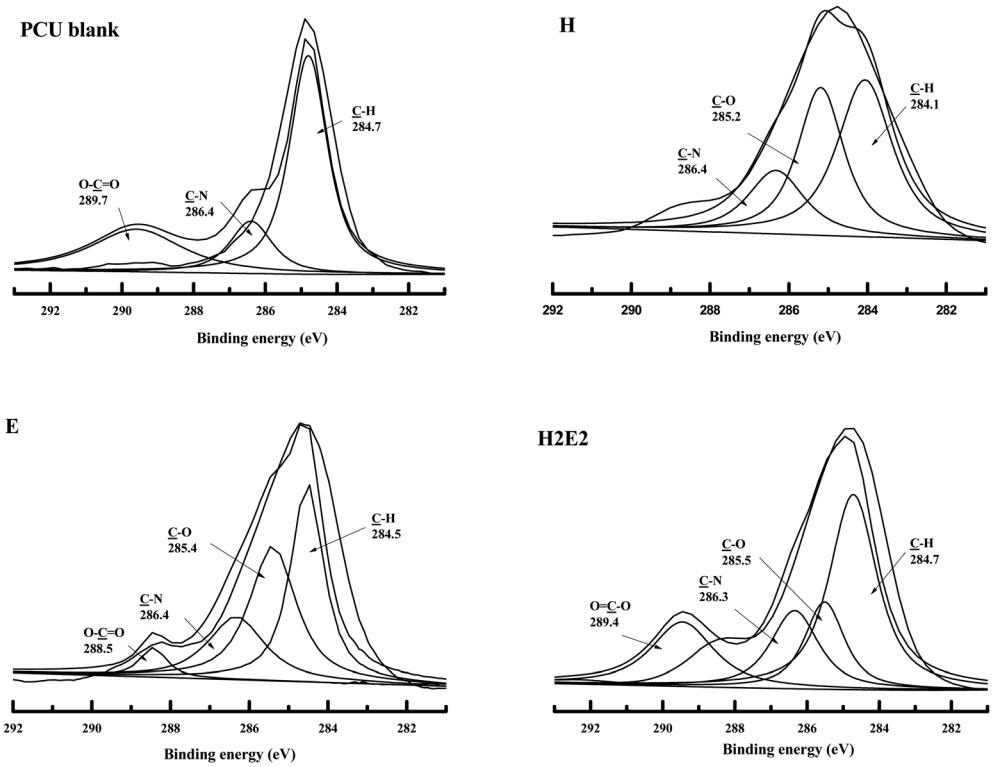


Fig. 1 The C 1s narrow spectra of PCU blank, H, E and H2E2 surfaces. H, E and H2E2 surfaces are the abbreviations of PCU-*g*-poly(HPMA4-*co*-EgMA0), PCU-*g*-poly(HPMA0-*co*-EgMA4) and PCU-*g*-poly(HPMA2-*co*-EgMA2), respectively.

group concentration was subtracted from the total to obtain the immobilized REDV concentration as well as the number of peptide units per unit area ($cm^{-2}$), as given in Table 2.

E-REDV surface had a relatively high REDV concentration ($15.6 \pm 1.2$ nmol $cm^{-2}$) due to the high EgMA content in the grafted copolymer, which acted as the bridge for the immobilization of the REDV peptide. The more EgMA molecules on the surface, the more reaction points were available for the REDV peptide to be conjugated.

### 3.2. Hydrophilicity of modified PCU-films

The surface hydrophilicity of modified PCU-films was investigated using WCA and WU measurements. It is generally considered that a relatively lower WCA and a higher WU indicate better hydrophilicity of materials. Among the modified surfaces and the control surface, the PCU blank showed the highest hydrophobicity with a high WCA of about 104° (Fig. 2). When the surface was modified by grafting the homopolymer PHPMA as well as its copolymers, the surface hydrophilicity was significantly increased. In particular, the H surface, having many hydrophilic PHPMA brushes, had the lowest WCA, while EgMA moieties reduced the surface hydrophilicity compared with the

Table 2 Immobilized REDV concentrations on the modified surfaces

| | REDV peptide amount | |
|---|---|---|
| Sample ID | nmol $cm^{-2}$ | Number of REDV $cm^{-2} \times 10^{-15}$ |
| H3E1-REDV | $9.5 \pm 0.5$ | $5.7 \pm 0.3$ |
| H2E2-REDV | $11.4 \pm 1.3$ | $6.8 \pm 0.9$ |
| H1E3-REDV | $12.8 \pm 0.7$ | $7.7 \pm 0.4$ |
| E-REDV | $15.6 \pm 1.2$ | $9.3 \pm 0.7$ |

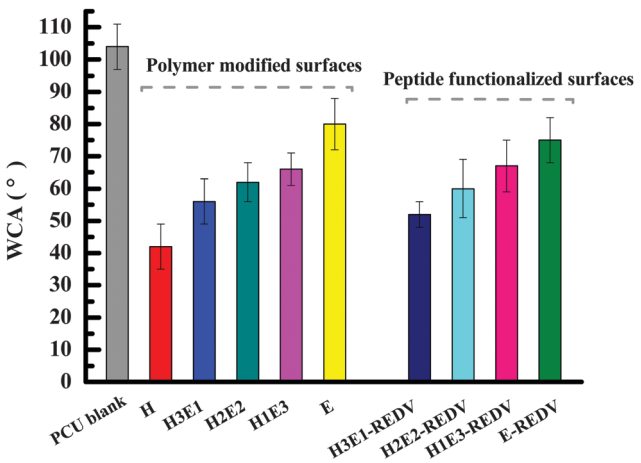


Fig. 2 WCA of different modified PCU-films. H, H3E1, H2E2, H1E3 and E surfaces are the abbreviations of PCU-*g*-poly(HPMA4-*co*-EgMA0), PCU-*g*-poly(HPMA3-*co*-EgMA1), PCU-*g*-poly(HPMA2-*co*-EgMA2), PCU-*g*-poly(HPMA1-*co*-EgMA3), and PCU-*g*-poly(HPMA0-*co*-EgMA4), respectively. H3E1-REDV, H2E2-REDV, H1E3-REDV and E-REDV surfaces are the peptide functionalized surfaces of PCU-*g*-poly(HPMA3-*co*-EgMA1)-REDV, PCU-*g*-poly(HPMA2-*co*-EgMA2)-REDV, PCU-*g*-poly(HPMA1-*co*-EgMA3)-REDV, and PCU-*g*-poly(HPMA0-*co*-EgMA4)-REDV, respectively. The PCU blank was used as the control. (Error bars represent mean ± SD).

 

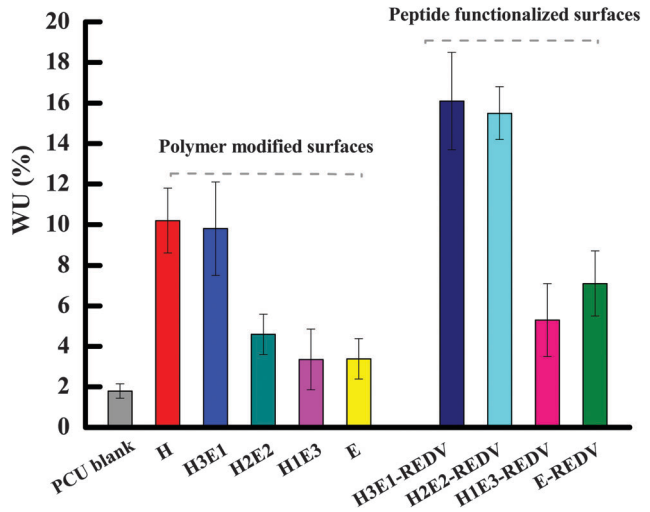


Fig. 3 WU (%) of different modified PCU-films after incubation at 37 °C for 24 h. H, H3E1, H2E2, H1E3 and E surfaces are the abbreviations of PCU-*g*-poly(HPMA4-*co*-EgMA0), PCU-*g*-poly(HPMA3-*co*-EgMA1), PCU-*g*-poly(HPMA2-*co*-EgMA2), PCU-*g*-poly(HPMA1-*co*-EgMA3) and PCU-*g*-poly(HPMA0-*co*-EgMA4), respectively. H3E1-REDV, H2E2-REDV, H1E3-REDV and E-REDV surfaces are the peptide functionalized surfaces of PCU-*g*-poly(HPMA3-*co*-EgMA1)-REDV, PCU-*g*-poly(HPMA2-*co*-EgMA2)-REDV, PCU-*g*-poly(HPMA1-*co*-EgMA3)-REDV, and PCU-*g*-poly(HPMA0-*co*-EgMA4)-REDV, respectively. A PCU blank was used as the control. (Error bars represent mean ± SD.)

H control because of the presence of the relatively hydrophobic eugenyl residues. The REDV peptide-functionalized PCU-films showed the same tendency; furthermore, their hydrophilicity was relatively higher than their parent surfaces. This is due to the linking of hydrophilic REDV peptide to EgMA moieties on the surfaces of poly(HPMA-*co*-EgMA) copolymers.

The WU of different modified PCU-films was evaluated after 24 h incubation in PBS (pH 7.4) at physiological temperature (37 °C) (Fig. 3). The WU values of H (10.2%) and H3E1 (9.8%) surfaces were relatively high because they had high content of hydrophilic HPMA on the modified surfaces. After peptide functionalization, the modified surfaces showed even higher WU values, for example, H3E1-REDV adsorbed 16.1% water. H2E2-REDV exhibited significantly increased surface hydrophilicity with a 15.5% WU, while before peptide functionalization H2E2 had a low WU of 4.58%. The water adsorption capacity increased with increasing hydrophilic peptide content on the surfaces. On the other hand, relatively hydrophobic EgMA moieties were responsible for a decrease in WU from H3E1 to H1E3 and from H3E1-REDV to H1E3-REDV surfaces. This tendency was associated with an increase in hydrophobicity with this monomer because it contains a hydrophobic aromatic ring.[68]

### 3.3. *In vitro* hemocompatibility test

As platelet adhesion plays an important role in the formation of thrombosis and inflammation, the hemocompatibility of different modified PCU-films was assessed *via* a platelet adhesion assay. If the interactions between platelets and biomaterial surfaces are very weak, few platelets will adhere and the adhered platelets may maintain their discoidal shape with a small spreading area. Conversely, if the interactions are too strong, platelets will be activated with spreading and aggregated morphologies.

The platelet adhesion on different modified PCU-films was investigated by SEM and the adhered platelets were quantified by manual counting and are summarized in Fig. 4. We could clearly see large quantities of platelets adhered on the PCU blank, and most of the adhered platelets were gathered and deformed, which indicated that these platelets were activated. In contrast, the H surface had the lowest number of adhered platelets and these platelets had maintained their discoidal shape. The REDV peptide functionalized surfaces showed significantly lower platelet adhesion than the PCU control. Furthermore, the number of adhered platelets on the modified surfaces decreased with increasing hydrophilic HPMA content on the surfaces. These results demonstrated that surface hydrophilicity plays an important role in inhibiting platelet adhesion and that the modification led to an improvement in surface hemocompatibility.

From the abovementioned observations, it can be concluded that PHPMA modified PCU-film could significantly decrease platelet adhesion, but very strong repelling ability would also negatively affect the adhesion of cells on biomaterial surfaces.[78] Thus, we prepared a series of poly(HPMA-*co*-EgMA) modified PCU-films with different ratios of HPMA and REDV in the copolymers. In the following cell experiments, we will investigate the effects of these modified surfaces on EC adhesion and growth to find the optimum ratio of PHPMA and REDV.

### 3.4. Adhesion, spreading and proliferation of HUVECs and HASMCs on modified surfaces

The surface chemical structures and hydrophilic properties significantly influence the adhesion, spreading and proliferation of ECs and further affect endothelialization. The preferential cell behaviors of HUVECs and HUASMCs on different modified PCU-films were evaluated using the FDA fluorescence staining method with different culture times (1, 3 and 7 days). Fluorescence micrographs, cell density results and surface coverage of HUVECs on different modified surfaces are shown in Fig. 5. The average number of cells was converted to cell density. The PCU blank, H and E surfaces were used as controls.

It was found that HUVEC numbers on all the surfaces increased along with the culture time. At the same culture time, H2E2-REDV and H1E3-REDV surfaces adhered more cells than other surfaces. These moderately hydrophilic surfaces were beneficial for cell growth; furthermore, REDV peptides were prone to adhering HUVECs. Conversely, the H surface had the lowest number of HUVECs owing to its high surface hydrophilicity. On the first day, HUVEC adhesion on the REDV peptide modified surfaces was enhanced, except for the H3E1-REDV surface. This is also due to the antifouling properties of HPMA and a relatively low REDV peptide content on the modified surface. After a 3 day culture, the number of HUVECs appeared obviously different, which could further be

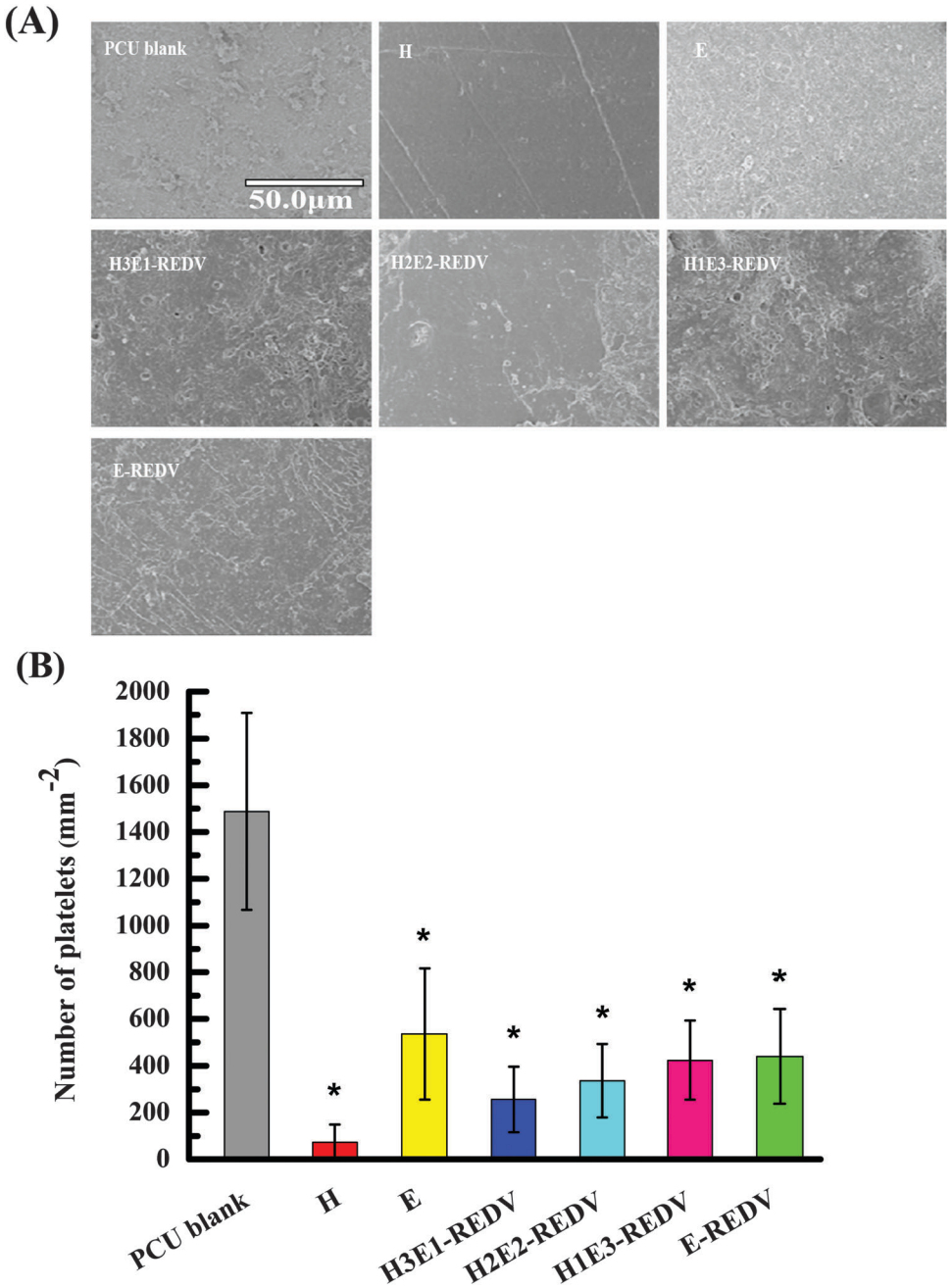


Fig. 4 Platelet adhesion on different PCU-films when in contact with PRP for 2 h: the SEM micrographs (A) and the statistical result (B), where H, E, H3E1-REDV, H2E2-REDV, H1E3-REDV, and E-REDV denote PCU-*g*-poly(HPMA4-*co*-EgMA0), PCU-*g*-poly(HPMA0-*co*-EgMA4), PCU-*g*-poly(HPMA3-*co*-EgMA1)-REDV, PCU-*g*-poly(HPMA2-*co*-EgMA2)-REDV, PCU-*g*-poly(HPMA1-*co*-EgMA3)-REDV, and PCU-*g*-poly(HPMA0-*co*-EgMA4)-REDV surfaces. A PCU blank was used as the control. The REDV peptide functionalized surfaces showed relatively lower platelet adhesion than the PCU blank. (Error bars represent mean ± SD. $*P < 0.05$ *vs.* the PCU blank.)

confirmed from the statistical results (Fig. 5B). After a 7 day culture, we could find a significant increase in the HUVEC number on all the REDV modified surfaces, especially on the H2E2-REDV and H1E3-REDV surfaces. Furthermore, the H1E3-REDV surface had the highest cell coverage area of 39.8%, which could be attributed to the interplay between the wettability of HPMA and the cell adhesion of the REDV peptide (Fig. 5C). These results confirmed that the REDV peptide modified surfaces were highly beneficial for HUVEC adhesion and proliferation.

The results of HASMCs on different PCU-films are shown in Fig. 6. On the first day of culture, the PCU blank and E control surfaces were found to have relatively more cells than other surfaces. For REDV peptide modified surfaces, the number of HASMCs on the surfaces increased only slightly with a decrease in the HPMA moiety. HASMC adhesion on these surfaces

 

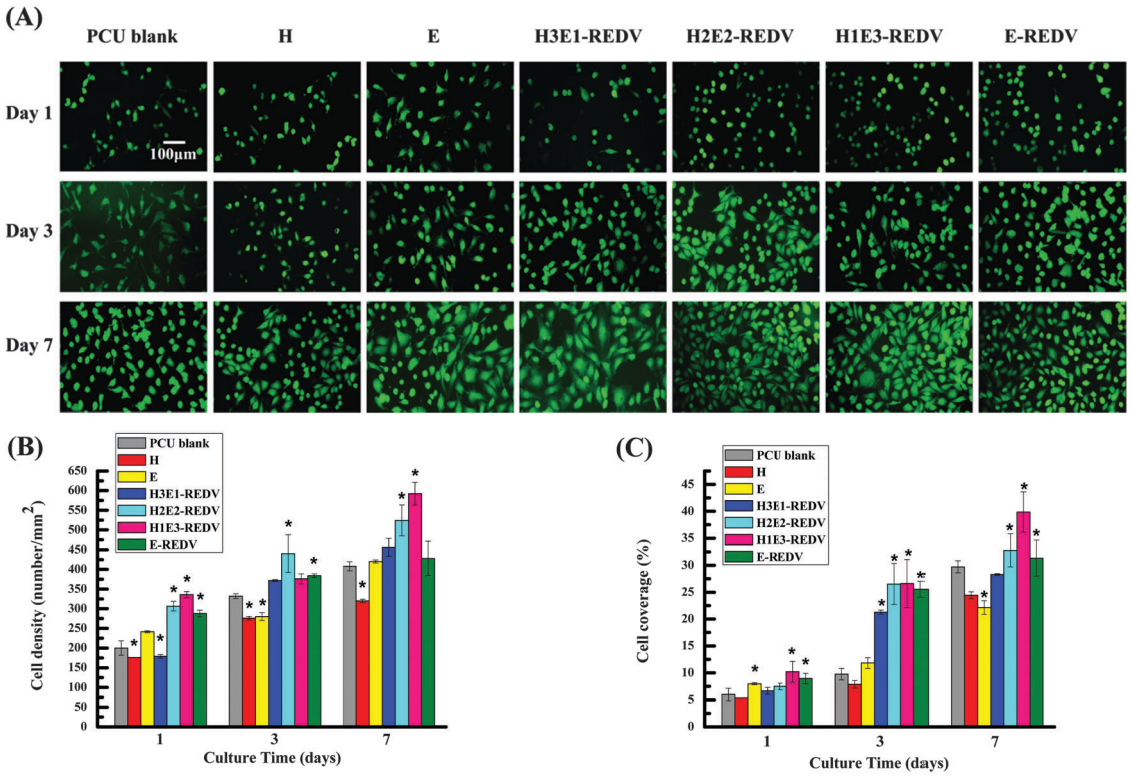


Fig. 5 Adhesion and proliferation of HUVECs on different PCU-films for 1, 3 and 7 day cultures. Fluorescence micrographs (A), cell density results (B), and surface coverage (%) (C) varied with different PCU-films and culture time, where H, E, H3E1-REDV, H2E2-REDV, H1E3-REDV and E-REDV surfaces are denoted as PCU-*g*-poly(HPMA4-*co*-EgMA0), PCU-*g*-poly(HPMA0-*co*-EgMA4), PCU-*g*-poly(HPMA3-*co*-EgMA1)-REDV, PCU-*g*-poly(HPMA2-*co*-EgMA2)-REDV, PCU-*g*-poly(HPMA1-*co*-EgMA3)-REDV, and PCU-*g*-poly(HPMA0-*co*-EgMA4)-REDV, respectively. The statistical result demonstrated that H2E2-REDV and H1E3-REDV surfaces showed relatively higher cell densities and cell coverage for HUVECs than the PCU blank control, H and E groups. (Error bars represent mean ± SD. $*P < 0.05$ *vs.* the PCU blank.)

mainly depends on the surface hydrophilic and hydrophobic balance, but not on REDV peptide. Because REDV peptide can only specifically adhere ECs, it is not beneficial for HASMC adhesion and growth. To understand the effects of REDV modified surfaces on the proliferation of HUVECs and HASMCs, we calculated the cell density curves, which are shown in Fig. 7(A)–(E). For the PCU blank, the growth tendency of HUVECs and HASMCs was similar; both cells showed an increased tendency in cell number during the culture period. Moreover, for REDV modified surfaces, HUVECs proliferated more rapidly but HASMCs increased with a mild growth. The cell number on the first day culture confirmed the specifically selective REDV peptide for HUVEC adhesion, because the number of HUVECs on the REDV modified surfaces was considerably higher than that of HASMCs. After 7-day culture, the proliferation of HUVECs and HASMCs on different PCU-films was significantly different. The ratios of HUVECs to HASMCs on the PCU blank, H3E1-REDV, H2E2-REDV, H1E3-REDV and E-REDV surfaces were 0.91, 1.70, 2.19, 2.21 and 1.37, respectively (Fig. 7(F)). The density of HUVECs on these REDV modified surfaces increased faster than that of HASMCs, especially for the H2E2-REDV and H1E3-REDV surfaces. All of these results further confirmed the adhesion selectivity of REDV peptide for HUVECs. The copolymer and REDV peptide functionalized surfaces showed an enhanced effect on the proliferation of HUVECs.

The morphologies of HUVECs and HASMCs on the modified PCU-films after a 3 day culture are shown in the ESI† (Fig. S1). Both HUVECs and HASMCs appeared to spread, flatten and grow on the PCU blank. Moreover, on the REDV modified surfaces, HUVECs formed bridges, spread well, and appeared multi-angular and robust. However, HASMCs did not spread well and shrank on these surfaces, which could also be verified by the surface coverage (32.8% for HUVECs (Fig. 5(C)) *vs.* 26.1% for HASMCs (Fig. 6(C)) on the H2E2-REDV surface). These results demonstrated that the REDV modified surfaces, especially H2E2-REDV and H1E3-REDV, selectively promoted the adhesion, spreading and proliferation of HUVECs.

For rapid endothelialization, biomaterial surfaces should promote good adhesion, spreading and proliferation of the ECs; furthermore, the adhered ECs should also maintain their viability and biofunctions. Herein, we used an MTT assay to assess the cell viability of HUVECs and HASMCs after a 3 day culture. The cell viability data of the blank control was defined as 100%. As shown in Fig. 8, all the surfaces except the H control showed high cell viabilities for both HUVECs and HASMCs. This was because of the high hydrophilicity of HPMA on the H surface. For REDV modified PCU, the viability of these

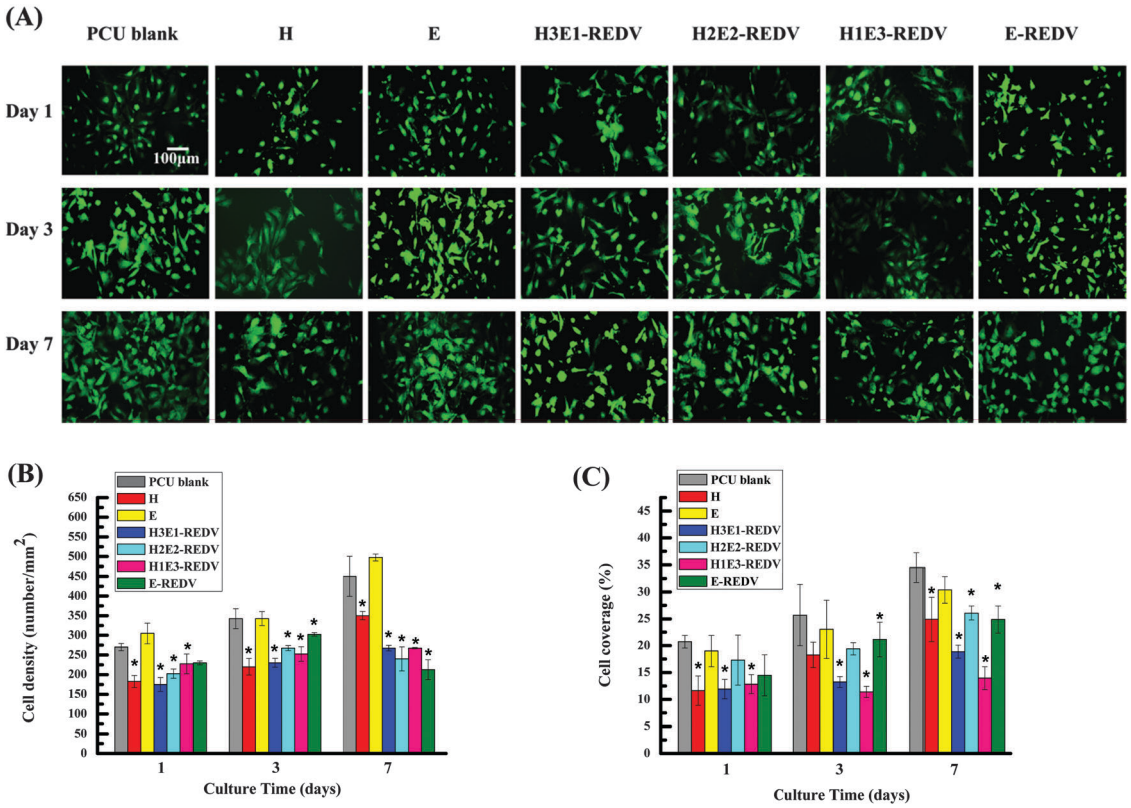


Fig. 6 Adhesion and proliferation of HASMCs on different PCU-films for 1, 3 and 7 day cultures. Fluorescence micrographs (A), cell density results (B), and surface coverage (%) (C) varied with different PCU-films and culture time, where H, E, H3E1-REDV, H2E2-REDV, H1E3-REDV and E-REDV surfaces represent PCU-*g*-poly(HPMA4-*co*-EgMA0), PCU-*g*-poly(HPMA0-*co*-EgMA4), PCU-*g*-poly(HPMA3-*co*-EgMA1)-REDV, PCU-*g*-poly(HPMA2-*co*-EgMA2)-REDV, PCU-*g*-poly(HPMA1-*co*-EgMA3)-REDV, and PCU-*g*-poly(HPMA0-*co*-EgMA4)-REDV, respectively. The REDV peptide functionalized surfaces showed relatively lower cell density and cell coverage for HASMCs than the PCU blank group. (Error bars represent mean ± SD. * $P < 0.05$ *vs.* the PCU blank.)

two types of cells was similar, except that the H2E2-REDV surface exhibited a statistical difference between HUVECs and HASMCs, showing that the H2E2-REDV surface could selectively promote HUVEC growth.

### 3.5. Co-culture of HUVECs and HASMCs

To investigate the effect of REDV peptide and HPMA on the competitive adhesion of HUVECs and HASMCs, we co-cultured HUVECs and HASMCs in the presence of modified PCU-films. The two types of cells were pre-stained with different cell-tracker dyes prior to mixing, *i.e.* HUVECs were stained by FDA with green fluorescence, whereas HASMCs were stained by CMTMR with red fluorescence. The images for the initial cell adhesion on different PCU-films were obtained after 2 h of co-culture. The fluorescence micrographs are shown in Fig. 9(A). Images at five different positions from three parallel experiments were obtained for each sample, and two different channels were selected for the same position. The cell number was calculated and converted to the numbers of these two types of cells on different PCU-films (Fig. 9(B)). The ratios of HUVECs to HASMCs adhered on PCU blank, H, E, H3E1-REDV, H2E2-REDV, H1E3-REDV, and E-REDV surfaces were 0.94, 0.68, 0.95, 1.76, 3.11, 1.72 and 1.25, respectively (Fig. 9(C)). The PCU blank had similar numbers of HUVECs and HASMCs, while both types of cells significantly decreased on the H surface because of its high hydrophilicity. The REDV modified surfaces adhered more HUVECs than HASMCs, and the tendency was significant, especially for the H2E2-REDV surface with a value of 3.11 (ratio of HUVECs to HASMCs). The REDV modified surfaces enhanced the initial competitive adhesion of HUVECs over HASMCs, which was preferential for rapid endothelialization.

### 3.6. Antimicrobial performance of the modified PCU-films

The antimicrobial activity of different modified PCU-films was qualitatively and quantitatively studied against *E. coli* by the direct contact method. The qualitative results are shown in Fig. 10. When the samples were in direct contact with bacteria, only the samples containing EgMA were capable of inhibiting bacterial growth, or at least delaying colony formation on them. The inhibitory effect was enhanced with increasing EgMA moieties of poly(HPMA-*co*-EgMA) on the surfaces, as could be clearly observed from H3E1-REDV (obvious colony), H2E2-REDV (almost no colony), H1E3-REDV (almost no colony), and E-REDV (almost no colony). This is due to the hydrophobic properties, together with the 4-allyl group of EgMA, enabling these surfaces to inhibit colony growth.[68] In contrast, for the

 

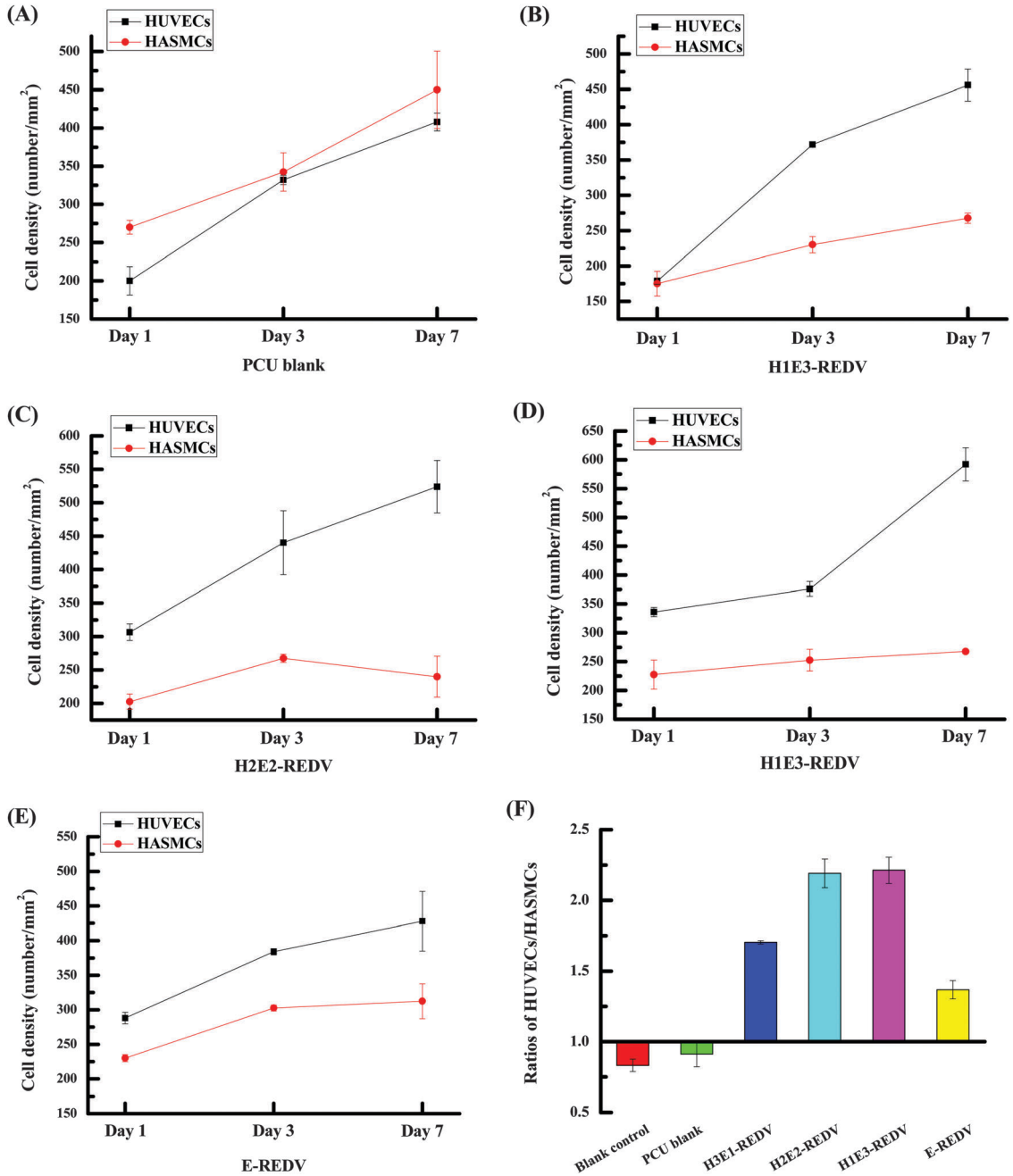


Fig. 7 Cell density curves of HUVECs and HASMCs on different PCU-films after 1, 3 and 7 day culture (A)–(E) and the density ratios of HUVECs/HASMCs on the 7th day (F), where H3E1-REDV, H2E2-REDV, H1E3-REDV, and E-REDV represent PCU-*g*-poly(HPMA3-*co*-EgMA1)-REDV, PCU-*g*-poly(HPMA2-*co*-EgMA2)-REDV, PCU-*g*-poly(HPMA1-*co*-EgMA3)-REDV, and PCU-*g*-poly(HPMA0-*co*-EgMA4)-REDV, respectively. A PCU blank was used as the control. REDV peptide functionalized surfaces, especially H2E2-REDV and H1E3-REDV surfaces, were more favorable for the growth and proliferation of HUVECs than HASMCs, while the PCU blank control showed the opposite results. (Error bars represent mean ± SD.)

PCU blank and the H control, bacterial growth inhibition was not observed and colonies were formed both beneath and around them.

To quantitatively evaluate the antimicrobial performance of different PCU-films, the samples were incubated with $3 \times 10^4$ CFU of *E. coli* for 3 h. Then, 10.0 μL of the inoculum was withdrawn and spread on agar plates, and the colonies formed were counted. The CFU count results are shown in Fig. 11(A). A significantly low colony number was observed on the agar plate for culture on the E, H2E2-REDV, H1E3-REDV and E-REDV surfaces. Moreover, bacterial cells grew quickly on the PCU blank and H control surfaces to produce colony counts of $2.9 \times 10^8$ and $2.8 \times 10^8$ CFU per mL, respectively. This indicated that EgMA provided the modified PCU-films with antibacterial properties. When the samples were immersed in a bacterial suspension for 12 h, the optical density (OD600) of the

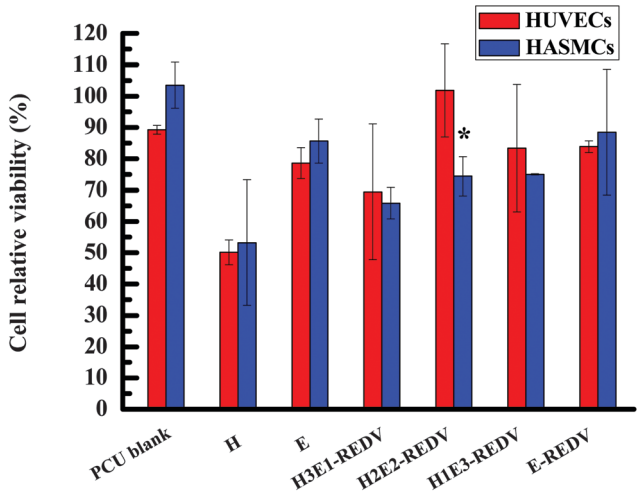


Fig. 8 Relative viability of HUVECs and HASMCs after a 3 day culture, where the H, E, H3E1-REDV, H2E2-REDV, H1E3-REDV and E-REDV surfaces represent PCU-*g*-poly(HPMA4-*co*-EgMA0), PCU-*g*-poly(HPMA0-*co*-EgMA4), PCU-*g*-poly(HPMA3-*co*-EgMA1)-REDV, PCU-*g*-poly(HPMA2-*co*-EgMA2)-REDV, PCU-*g*-poly(HPMA1-*co*-EgMA3)-REDV, and PCU-*g*-poly(HPMA0-*co*-EgMA4)-REDV, respectively. H2E2-REDV, H1E3-REDV and E-REDV groups maintained growth of both cells above 70%. However, both H and H3E1-REDV groups exhibited poor cell viability (less than 70%) because of the high hydrophilicity of the HPMA moieties. Only the H2E2-REDV surface exhibited a statistical difference between HUVECs and HASMCs, further indicating that this surface is beneficial for the selective enhancement of HUVEC growth. (Error bars represent mean ± SD.)

suspension was used to characterize the bacterial concentration. The PCU blank and H control could not inhibit bacterial growth (Fig. 11(B)), but E, H2E2-REDV, H1E3-REDV and E-REDV surfaces showed high antibacterial activity with low OD600 values. These results confirm that the antimicrobial activity of EgMA is retained after immobilization. The H2E2-REDV, H1E3-REDV, and E-REDV surfaces possessed good antimicrobial properties.

## 4. Discussion

Nowadays, vascular stents and grafts are usually applied for the treatment of coronary and peripheral artery diseases.[3] However, restenosis, thrombosis, and bacterial infection often cause implant failure. Therefore, to design and develop an ideal vascular implant, mechanical and biological factors have become major concerns. First of all, excellent flexibility and strength of the biomaterials are the basic requirements for vascular grafts. They must tolerate the force imposed by the blood flow, avoid the recoil and support vascular remodeling. Second, biomaterials should possess superior hemocompatibility and have antithrombotic properties. When the implant surface is in direct contact with blood, plasma proteins are prone to be adsorbed on the exposed surface. The adsorption and denaturation of some plasma proteins can cause the subsequent adhesion and activation of platelets, which trigger the coagulation cascade and inflammatory reactions, finally resulting in restenosis and thrombosis. Third, the surface should be beneficial for endothelialization. The entire natural vascular system is protected by a non-thrombogenic lining of ECs; thus, the EC layer plays an important role in preserving the high patency of artificial vascular grafts. Last but not least, antibacterial properties should also be taken into consideration because infections caused by the adhered bacterial cells during an operation are a major problem in clinical applications.

PCU materials have an elastic modulus of 1.3 MPa, which is four times stronger than the coronary artery.[70] The compliance value of PCU was tested to be about 8.1 percent per mmHg $\times 10^{-2}$, similar to that of the artery (8.0 percent per mmHg $\times 10^{-2}$).[5] The burst pressure of porous polyurethane grafts was found to be 1850–2050 mmHg, considerably greater than that of other grafts.[79] Owing to their excellent mechanical and physical properties, PCU materials have been widely applied in vascular applications and relevant fields. However, the long-term application is still limited due to insufficient hemocompatibility, potential thrombosis and restenosis. Surface modification, as a simple and convenient method of improving surface properties, was used here to overcome these severe problems. First of all, the copolymers of hydrophilic HPMA and antimicrobial EgMA were used to modify PCU surfaces with the aim of improving both hemocompatibility and antibacterial properties. As a robust method, the ARGET ATRP technique was applied here to endow the stable modified surface with controllable properties. Then, photo-initiated thiol–ene click chemistry was used to conjugate cysteine-terminated CREDV peptide to the pendant double bonds on poly(HPMA-*co*-EgMA) modified PCU films to improve the selective adhesion and proliferation of ECs. The thiol–ene click reaction also provided a convenient and stable method for the conjugation of biological moieties. The hydrophilic poly(HPMA-*co*-EgMA) copolymers could increase the surface wettability, which was demonstrated by the decreased WCA (Fig. 2). Surface wettability is related to fouling resistance. The H surface contains highly hydrophilic PHPMA, which can inhibit platelet adhesion; this was confirmed by the lowest number of adhered platelets. Although high wettability can effectively prevent protein adsorption on biomaterial surfaces, it can also lead to decreased cell adhesion. For example, neither ECs nor SMCs can adhere and proliferate efficiently on the H surface. We adjusted the surface hydrophilicity by grafting poly(HPMA-*co*-EgMA) copolymers with different ratios of HPMA and EgMA. The moderate hydrophilicity is beneficial for cell adhesion and migration. Furthermore, cell adhesive peptides have usually been used to modify biomaterial surfaces to improve cell adhesion. Among cell adhesive peptides, REDV peptide can selectively adhere ECs. Thus, we used CREDV peptide to modify the surfaces for improving EC adhesion and hemocompatibility. Besides, the surface modified PCU maintained its intrinsic mechanical properties, such as high elastic modulus and burst pressure.

To improve the long-term patency of artificial vascular grafts, endothelialization on the graft surface is often enhanced by various approaches. The endothelialization processes on

 

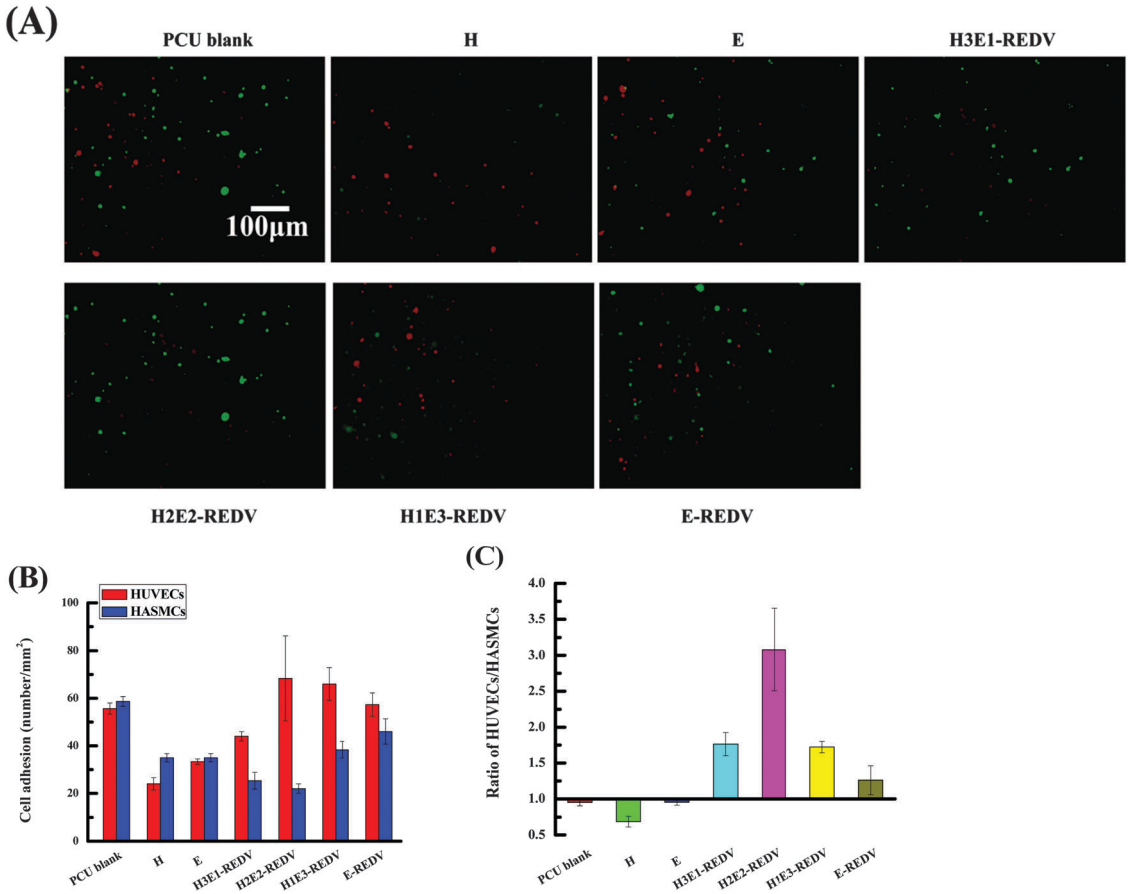


Fig. 9 Co-culture of HUVECs and HASMCs on REDV functionalized PCU-films after 2 h incubation. Fluorescence micrographs (A) were obtained with a Fluorescence Olympus U-RFLT50 microscope and an Olympus DP72 microscope. HUVECs were stained green and HASMCs were stained red. Cell adhesion numbers (B) were obtained by manual counting, and the ratio of HUVEC/HASMC density (C) was calculated from (B), where H, E, H3E1-REDV, H2E2-REDV, H1E3-REDV and E-REDV surfaces are PCU-*g*-poly(HPMA4-*co*-EgMA0), PCU-*g*-poly(HPMA0-*co*-EgMA4), PCU-*g*-poly(HPMA3-*co*-EgMA1)-REDV, PCU-*g*-poly(HPMA2-*co*-EgMA2)-REDV, PCU-*g*-poly(HPMA1-*co*-EgMA3)-REDV, and PCU-*g*-poly(HPMA0-*co*-EgMA4)-REDV, respectively. The REDV peptide functionalized surfaces, especially H2E2-REDV, showed higher adhesion for HUVECs than for HASMCs. However, the PCU blank and H and E surfaces showed the opposite results. (Error bars represent mean ± SD.)

artificial vascular grafts involve many complex processes such as EC adhesion, migration and proliferation, which are regulated by numerous signals. The interactions between ECs and SMCs in blood vessel walls may control the growth and function of blood vessels. The adhesion, spread, migration and proliferation of ECs must compete with and involve other cells. The growth and proliferation of various cells, especially SMCs, may interfere with ECs, which could further affect rapid endothelialization. To mimic the properties of native tissues for promoting endothelialization, Ji *et al.*[53,74,80] modified stents with hydrophilic components such as poly(ethylene glycol), phosphorylcholine or polycarboxybetaine as well as the EC specific adhesion peptide, REDV. The functionalized stents could effectively enhance the competitive growth of ECs over SMCs. In our study, the adhesion and proliferation of HUVECs and HASMCs were investigated in a solo-culture system for 1, 3 and 7 days and in a co-culture system for 2 h to study the effects of HPMA and REDV peptide on endothelialization (especially initial cell adhesion). Our results demonstrated that poly(HPMA-*co*-EgMA)-REDV modified surfaces enhanced the adhesion and proliferation of HUVECs but suppressed the behaviors of HASMCs. In particular, for poly(HPMA-*co*-EgMA)-REDV with a HPMA and EgMA molar ratio of 1 : 3, the ratio of HUVECs to HASMCs could reach 2.21 on the 7th day in a solo-culture, and the initial adhesion of HUVECs was also relatively high after 2 h co-culture. REDV peptide can specifically bind to $\alpha_4\beta_1$ integrin, which is abundant on ECs, whereas scarce on SMCs. It specifically adsorbs ECs rather than SMCs. The selective adhesion and proliferation of HUVECs is facilitated from the synergistic effects of hydrophilic HPMA and REDV peptide on the surfaces.

For addressing bacterial infection after operations, one strategy is to prepare ultra-low fouling surfaces on implants with the aim of effectively preventing bacterial adhesion, whereas another involves using active moieties to kill the attached bacterial cells.[8] PHPMA modified biomaterial surfaces show ultra-low fouling properties and they can effectively prevent protein adsorption when in contact with blood. However, PHPMA cannot kill bacteria once they are adhered on the implant surface.[34] Recently, the antimicrobial and anti-inflammatory properties of

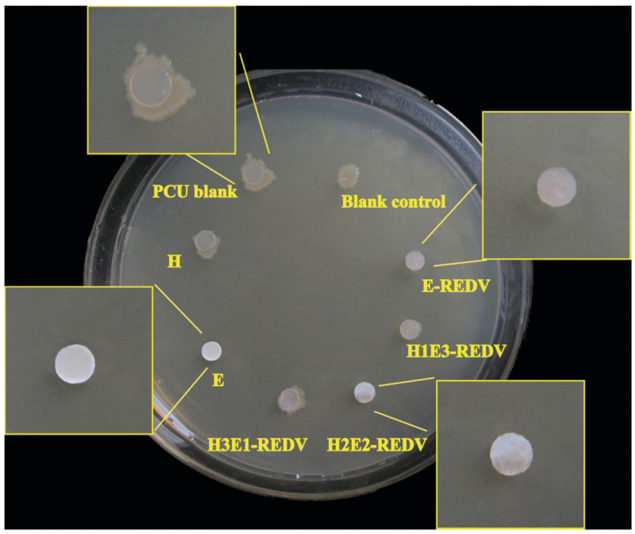


Fig. 10 Qualitative evaluation of antimicrobial effects of different PCU-films by *E. coli* colony formation tests after 24 h incubation at 37 °C, where H, E, H3E1-REDV, H2E2-REDV, H1E3-REDV and E-REDV surfaces are PCU-*g*-poly(HPMA4-*co*-EgMA0), PCU-*g*-poly(HPMA0-*co*-EgMA4), PCU-*g*-poly(HPMA3-*co*-EgMA1)-REDV, PCU-*g*-poly(HPMA2-*co*-EgMA2)-REDV, PCU-*g*-poly(HPMA1-*co*-EgMA3)-REDV, and PCU-*g*-poly(HPMA0-*co*-EgMA4)-REDV, respectively. The PCU blank, H and E surfaces, as well as the blank group without films were used as the controls.

eugenol have attracted considerable attention.[66,67] The acrylate derivative of EgMA and its homopolymer or copolymers also show superior antibacterial properties. In this study, we combined these two strategies using the copolymers of poly(HPMA-*co*-EgMA) to modify the PCU surface. HPMA as the antifouling moiety and EgMA as the antimicrobial moiety can provide the surface with both antifouling and antimicrobial properties. The antibacterial assay results demonstrated that the EgMA immobilized surfaces have effective antibacterial activity, consistent with previous reports.[68,69] More importantly, poly(HPMA-*co*-EgMA)-REDV modified surfaces possess multiple functions such as excellent hemocompatibility, specific adhesion and proliferation of ECs, as well as antibacterial properties. These multiple functions are beneficial for vascular graft biomaterials.

## 5. Conclusion

We have developed a multifunctional surface with hydrophilic HPMA, antibacterial EgMA and EC adhesive REDV peptide on PCU to selectively promote endothelialization. First, different monomer ratios of HPMA and EgMA were grafted onto PCU-film by an ATRP technique to modulate the surface hydrophilicity. Second, cysteine-terminated CREDV peptide was conjugated with the pendant double bonds on the modified PCU-film by photo-initiated thiol–ene click chemistry. By varying HPMA and EgMA ratios in the feed, we found that a high amount of HPMA (such as in H, H3E1, H2E2 and their corresponding REDV peptide modified surfaces) could effectively enhance hemocompatibility. REDV peptide enhanced the competitive growth of HUVECs over HASMCs on the hydrophilic surfaces. Furthermore, antibacterial EgMA could inhibit bacteria-induced infection. The successful fabrication of multifunctional biomaterial surfaces with excellent hemocompatibility and endothelialization, as well as effective antimicrobial activity, through a feasible route could be an attractive platform for tissue engineering applications.

## Acknowledgements

This project was supported by the National Natural Science Foundation of China, China (Grant No. 31370969), the International Cooperation from Ministry of Science and Technology of China, China (Grant No. 2013DFG52040), and the Program of Introducing Talents of Discipline to Universities of China, China (No. B06006).

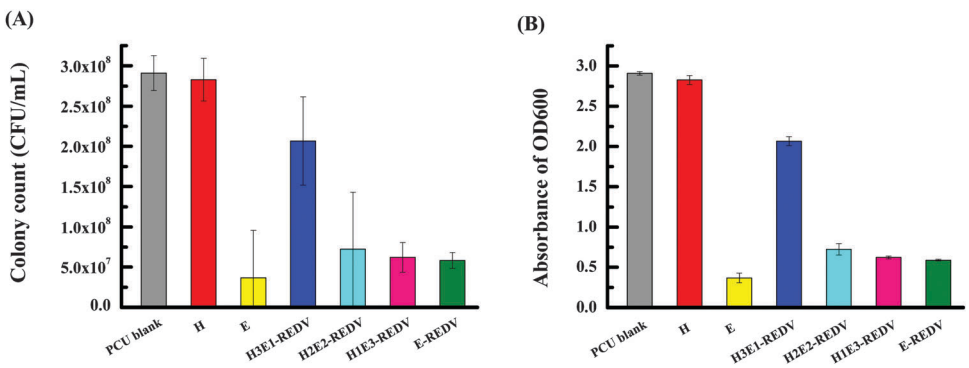


Fig. 11 Antimicrobial activities of different PCU-films against *E. coli* after 3 h incubation, determined by CFU counting after incubating the bacterial suspension with different PCU-films (A) and optical density (OD600) measurements of LB medium after overnight incubation with different PCU-films containing remaining bacterial suspension (B). H, E, H3E1-REDV, H2E2-REDV, H1E3-REDV and E-REDV surfaces are PCU-*g*-poly(HPMA4-*co*-EgMA0), PCU-*g*-poly(HPMA0-*co*-EgMA4), PCU-*g*-poly(HPMA3-*co*-EgMA1)-REDV, PCU-*g*-poly(HPMA2-*co*-EgMA2)-REDV, PCU-*g*-poly(HPMA1-*co*-EgMA3)-REDV, and PCU-*g*-poly(HPMA0-*co*-EgMA4)-REDV, respectively. The H2E2-REDV, H1E3-REDV and E-REDV surfaces demonstrated good antimicrobial activity compared with the E surface. (Error bars represent mean ± SD.)

 

## References


1 A. de Mel, G. Jell, M. M. Stevens and A. M. Seifalian, *Biomacromolecules*, 2008, **9**, 2969–2979.
2 J. L. Wang, B. C. Li, Z. J. Li, K. F. Ren, L. J. Jin, S. M. Zhang, H. Chang, Y. X. Sun and J. Ji, *Biomaterials*, 2014, **35**, 7679–7689.
3 P. Qi, S. Chen, T. Liu, J. Chen, Z. Yang, Y. Weng, J. Chen, J. Wang, M. F. Maitz and N. Huang, *Biointerphases*, 2014, **9**, 029017.
4 R. Zdrahala and I. Zdrahala, *J. Biomater. Appl.*, 1999, **14**, 67–90.
5 N. R. Tai, H. J. Salacinski, A. Edwards, G. Hamilton and A. M. Seifalian, *Br. J. Surg.*, 2000, **87**, 1516–1524.
6 D. V. Bax, A. Kondyurin, A. Waterhouse, D. R. McKenzie, A. S. Weiss and M. M. Bilek, *Biomaterials*, 2014, **35**, 6797–6809.
7 H. Ceylan, A. B. Tekinay and M. O. Guler, *Biomaterials*, 2011, **32**, 8797–8805.
8 L. Mi and S. Jiang, *Angew. Chem., Int. Ed. Engl.*, 2014, **53**, 1746–1754.
9 X. Ren, Y. Feng, J. Guo, H. Wang, Q. Li, J. Yang, X. Hao, J. Lv, N. Ma and W. Li, *Chem. Soc. Rev.*, 2015, **44**, 5680–5742.
10 P. Qi, M. F. Maitz and N. Huang, *Surf. Coat. Technol.*, 2013, **233**, 80–90.
11 E. Ostuni, R. G. Chapman, R. E. Holmlin, S. Takayama and G. M. Whitesides, *Langmuir*, 2001, **17**, 5605–5620.
12 S. Pasche, J. Voros, H. J. Griesser, N. D. Spencer and M. Textor, *J. Phys. Chem. B*, 2005, **109**, 17545–17552.
13 H. Y. Zhao, Y. K. Feng and J. T. Guo, *J. Appl. Polym. Sci.*, 2011, **119**, 3717–3727.
14 W. Yuan, Y. Feng, H. Wang, D. Yang, B. An, W. Zhang, M. Khan and J. Guo, *Mater. Sci. Eng., C*, 2013, **33**, 3644–3651.
15 J. Yang, J. Lv, M. Behl, A. Lendlein, D. Yang, L. Zhang, C. Shi, J. Guo and Y. Feng, *Macromol. Biosci.*, 2013, **13**, 1681–1688.
16 H. Y. Wang, Y. K. Feng, Z. C. Fang, W. J. Yuan and M. Khan, *Mater. Sci. Eng., C*, 2012, **32**, 2306–2315.
17 J. Lu, Y. K. Feng, B. Gao and J. T. Guo, *Macromol. Res.*, 2012, **20**, 693–702.
18 J. Lu, Y. K. Feng, B. Gao and J. T. Guo, *J. Polym. Res.*, 2012, **19**, 9959–9969.
19 M. Khan, J. Yang, C. Shi, Y. Feng, W. Zhang, K. Gibney and G. N. Tew, *RSC Adv.*, 2015, **5**, 11284–11292.
20 J. T. Guo, Y. K. Feng, Y. Q. Ye and H. Y. Zhao, *J. Appl. Polym. Sci.*, 2011, **122**, 1084–1091.
21 W. Gao, Y. K. Feng, J. Lu, M. Khan and J. T. Guo, *Macromol. Res.*, 2012, **20**, 1063–1069.
22 B. Gao, Y. Feng, J. Lu, L. Zhang, M. Zhao, C. Shi, M. Khan and J. Guo, *Mater. Sci. Eng., C*, 2013, **33**, 2871–2878.
23 Y. K. Feng, D. Z. Yang, M. Behl, A. Lendlein, H. Y. Zhao and J. T. Guo, *Macromol. Symp.*, 2011, **309–310**, 6–15.
24 Y. Feng, H. Zhao, M. Behl, A. Lendlein, J. Guo and D. Yang, *J. Mater. Sci.: Mater. Med.*, 2013, **24**, 61–70.
25 W. Zhou, Y. Feng, J. Yang, J. Fan, J. Lv, L. Zhang, J. Guo, X. Ren and W. Zhang, *J. Mater. Sci.: Mater. Med.*, 2015, **26**, 56.
26 H. Y. Wang, Y. K. Feng, H. Y. Zhao, R. F. Xiao, J. Lu, L. Zhang and J. T. Guo, *Macromol. Res.*, 2012, **20**, 347–350.
27 H. Y. Wang, Y. K. Feng, Z. C. Fang, R. F. Xiao, W. J. Yuan and M. Khan, *Macromol. Res.*, 2013, **21**, 860–869.
28 M. Q. Tan, Y. K. Feng, H. Y. Wang, L. Zhang, M. Khan, J. T. Guo, Q. L. Chen and J. S. Liu, *Macromol. Res.*, 2013, **21**, 541–549.
29 C. Shi, W. Yuan, M. Khan, Q. Li, Y. Feng, F. Yao and W. Zhang, *Mater. Sci. Eng., C*, 2015, **50**, 201–209.
30 A. Kelsch, S. Tomcin, K. Rausch, M. Barz, V. Mailander, M. Schmidt, K. Landfester and R. Zentel, *Biomacromolecules*, 2012, **13**, 4179–4187.
31 J. Kopecek and P. Kopeckova, *Adv. Drug Delivery Rev.*, 2010, **62**, 122–149.
32 K. Ulbrich, V. Subr, J. Strohalm, D. Plocova, M. Jelinkova and B. Rihova, *J. Controlled Release*, 2000, **64**, 63–79.
33 C. Rodriguez-Emmenegger, E. Brynda, T. Riedel, M. Houska, V. Subr, A. B. Alles, E. Hasan, J. E. Gautrot and W. T. Huck, *Macromol. Rapid Commun.*, 2011, **32**, 952–957.
34 F. Surman, T. Riedel, M. Bruns, N. Y. Kostina, Z. Sedlakova and C. Rodriguez-Emmenegger, *Macromol. Biosci.*, 2015, **15**, 636–646.
35 J. Chan, Y. Zhang and K. Uhrich, *Bioconjugate Chem.*, 2015, **26**, 1359–1369.
36 O. F. Khan and M. V. Sefton, *Trends Biotechnol.*, 2011, **29**, 379–387.
37 L. Yu, Y. Feng, Q. Li, X. Hao, W. Liu, W. Zhou, C. Shi, X. Ren and W. Zhang, *React. Funct. Polym.*, 2015, **91–92**, 19–27.
38 Q. Li, C. Shi, W. Zhang, M. Behl, A. Lendlein and Y. Feng, *Adv. Healthcare Mater.*, 2015, **4**, 1225–1235.
39 A. W. Feinberg, J. F. Schumacher and A. B. Brennan, *Acta Biomater.*, 2009, **5**, 2013–2024.
40 N. Salehi-Nik, G. Amoabediny, M. A. Shokrgozar, K. Mottaghy, J. Klein-Nulend and B. Zandieh-Doulabi, *Biomed. Mater.*, 2015, **10**, 015024.
41 T. Ren, S. Yu, Z. Mao, S. E. Moya, L. Han and C. Gao, *Biomacromolecules*, 2014, **15**, 2256–2264.
42 C. Chollet, C. Chanseau, M. Remy, A. Guignandon, R. Bareille, C. Labrugere, L. Bordenave and M. C. Durrieu, *Biomaterials*, 2009, **30**, 711–720.
43 K. Kanie, Y. Narita, Y. Zhao, F. Kuwabara, M. Satake, S. Honda, H. Kaneko, T. Yoshioka, M. Okochi, H. Honda and R. Kato, *Biotechnol. Bioeng.*, 2012, **109**, 1808–1816.
44 J. S. Miller, C. J. Shen, W. R. Legant, J. D. Baranski, B. L. Blakely and C. S. Chen, *Biomaterials*, 2010, **31**, 3736–3743.
45 S. T. Gould, N. J. Darling and K. S. Anseth, *Acta Biomater.*, 2012, **8**, 3201–3209.
46 M. H. Fittkau, P. Zilla, D. Bezuidenhout, M. P. Lutolf, P. Human, J. A. Hubbell and N. Davies, *Biomaterials*, 2005, **26**, 167–174.
47 C. Tang, F. Kligman, C. C. Larsen, K. Kottke-Marchant and R. E. Marchant, *J. Biomed. Mater. Res., Part A*, 2009, **88**, 348–358.
48 A. S. Gupta, G. Huang, B. J. Lestini, S. Sagnella, K. Kottke-Marchant and R. E. Marchant, *Thromb. Haemostasis*, 2005, **93**, 106–114.
49 B. D. Plouffe, M. Radisic and S. K. Murthy, *Lab Chip*, 2008, **8**, 462–472.

50 M. I. Castellanos, A. S. Zenses, A. Grau, J. C. Rodriguez-Cabello, F. J. Gil, J. M. Manero and M. Pegueroles, *Colloids Surf., B*, 2015, **127**, 22–32.
51 H. Wang, Y. Feng, J. Yang, J. Guo and W. Zhang, *J. Mater. Chem. B*, 2015, **3**, 3379–3391.
52 X. Hao, Q. Li, J. Lv, L. Yu, X. Ren, L. Zhang, Y. Feng and W. Zhang, *ACS Appl. Mater. Interfaces*, 2015, **7**, 12128–12140.
53 Y. Wei, Y. Ji, L. Xiao, Q. Lin and J. Ji, *Colloids Surf., B*, 2011, **84**, 369–378.
54 Z. Yang, Q. Tu, J. Wang and N. Huang, *Biomaterials*, 2012, **33**, 6615–6625.
55 H. Zhang, X. Jia, F. Han, J. Zhao, Y. Zhao, Y. Fan and X. Yuan, *Biomaterials*, 2013, **34**, 2202–2212.
56 Q. Lin, X. Ding, F. Qiu, X. Song, G. Fu and J. Ji, *Biomaterials*, 2010, **31**, 4017–4025.
57 J. Lv, X. F. Hao, J. Yang, Y. K. Feng, M. Behl and A. Lendlein, *Macromol. Chem. Phys.*, 2014, **215**, 2463–2472.
58 C. Shi, F. Yao, Q. Li, M. Khan, X. Ren, Y. Feng, J. Huang and W. Zhang, *Biomaterials*, 2014, **35**, 7133–7145.
59 C. C. Shi, F. L. Yao, J. W. Huang, G. L. Han, Q. Li, M. Khan, Y. K. Feng and W. C. Zhang, *J. Mater. Chem. B*, 2014, **2**, 1825–1837.
60 R. B. McFee, *DM, Dis.–Mon.*, 2009, **55**, 422–438.
61 K. Lim, R. R. Chua, H. Bow, P. A. Tambyah, K. Hadinoto and S. S. Leong, *Acta Biomater.*, 2015, **15**, 127–138.
62 M. Levi, *Cardiovasc. Res.*, 2003, **60**, 26–39.
63 M. Khan, Y. K. Feng, D. Z. Yang, W. Zhou, H. Tian, Y. Han, L. Zhang, W. J. Yuan, J. Zhang, J. T. Guo and W. C. Zhang, *J. Polym. Sci., Part A: Polym. Chem.*, 2013, **51**, 3166–3176.
64 K. Lim, R. R. Chua, R. Saravanan, A. Basu, B. Mishra, P. A. Tambyah, B. Ho and S. S. Leong, *ACS Appl. Mater. Interfaces*, 2013, **5**, 6412–6422.
65 D. Savoia, *Future Microbiol.*, 2012, **7**, 979–990.
66 L. Rojo, B. Vazquez, J. Parra, A. L. Bravo, S. Deb and J. S. Roman, *Biomacromolecules*, 2006, **7**, 2751–2761.
67 L. Rojo, B. Vazquez, J. S. Roman and S. Deb, *Dent. Mater.*, 2008, **24**, 1709–1716.
68 L. Rojo, J. M. Barcenilla, B. Vazquez, R. Gonzalez and J. S. Roman, *Biomacromolecules*, 2008, **9**, 2530–2535.
69 L. Rojo, A. Borzacchiello, J. Parra, S. Deb, B. Vazquez and J. S. Roman, *J. Mater. Sci.: Mater. Med.*, 2008, **19**, 1467–1477.
70 M. Khan, J. Yang, C. Shi, J. Lv, Y. Feng and W. Zhang, *Acta Biomater.*, 2015, **20**, 69–81.
71 M. Bhatia, M. Ahuja and H. Mehta, *Carbohydr. Polym.*, 2015, **131**, 119–124.
72 R. Sharma and M. Ahuja, *Carbohydr. Polym.*, 2011, **85**, 658–663.
73 C. K. Riener, G. Kada and H. J. Gruber, *Anal. Bioanal. Chem.*, 2002, **373**, 266–276.
74 Y. Wei, Y. Ji, L. L. Xiao, Q. K. Lin, J. P. Xu, K. F. Ren and J. Ji, *Biomaterials*, 2013, **34**, 2588–2599.
75 A. L. Carbone-Howell, N. D. Stebbins and K. E. Uhrich, *Biomacromolecules*, 2014, **15**, 1889–1895.
76 M. Wang, J. Lin, H. Tseng and S. Hsu, *ACS Appl. Mater. Interfaces*, 2012, **4**, 338–350.
77 M. Taylor, W. Eckenhoff and T. Pintauer, *Dalton Trans.*, 2010, **39**, 11475–11482.
78 D. P. Dowling, I. S. Miller, M. Ardhaoui and W. M. Gallagher, *J. Biomater. Appl.*, 2011, **26**, 327–347.
79 S. Sarkar, H. J. Salacinski, G. Hamilton and A. M. Seifalian, *Eur. J. Vasc. Endovasc. Surg.*, 2006, **31**, 627–636.
80 Y. Ji, Y. Wei, X. Liu, J. Wang, K. Ren and J. Ji, *J. Biomed. Mater. Res., Part A*, 2012, **100**, 1387–1397.

 